

ULTRASHORT LASER PULSE SHAPING AND CHARACTERIZATION FOR TAILORED ELECTRON BUNCH GENERATION *

T. Xu[†], P. Piot¹, Northern Illinois University, DeKalb, IL, USA
M.E. Conde, G. Ha, J.G. Power, Argonne National Laboratory, Lemont, IL, USA
¹also at Argonne National Laboratory, Lemont, IL, USA

Abstract

Temporally-shaped laser pulse are desirable in various applications including emittance reduction and beam-driven acceleration. Pulse-shaping techniques enable flexible controls over the longitudinal distribution of electron bunches emitted from photocathode. While direct manipulation and measurement of ultrashort pulses can be challenging in the time domain, both actions can be performed in the frequency domain. In this paper, we report investigations toward the development of laser shaper and diagnostics at the Argonne Wakefield Accelerator. Simulations are presented to describe the shaping and measurement process based on a digital mask and a frequency resolved optical gating method.

INTRODUCTION

Collinear wakefield accelerators have driven the demands for electron bunches with tailored current profiles [1]. It has been recognized that longitudinally asymmetric drive bunches produce higher transformer ratios and ultimately enable a larger energy transfer between drive and witness. Therefore bunch shaping techniques to produce asymmetric drive beams are crucial for efficient acceleration. One promising technique that could generate shaped electron bunches is laser shaping where laser pulses are temporally shaped before impinging on a photocathode [2–4]. Laser shaping technique is appealing owing to its simplicity and possible combination with other shaping techniques to produce precisely tailored electron bunches.

In the picosecond regime, laser pulse shaping can be realized by splitting pulses in birefringent crystal and stacking the replicae temporally [5]. This scheme often requires fine-tuning of the orientation of crystals and lacks versatility. Pulses are generated on a femtosecond time scale, providing broader spectral bandwidths compared with picosecond lasers. This allows the manipulation of different spectral components, hence the ability to generate arbitrary optical waveforms [6]. Complementary to laser shaper is the diagnostics for characterizing the pulse temporal distributions. Optoelectronic devices like streak cameras reach temporal resolutions of the order of 100 femtoseconds. Thus a different approach is required to characterize the shaped pulse.

In the present work, we describe our approach to develop a pulse shaper and associated temporal diagnostics at the Argonne Wakefield Accelerator (AWA) facility. The AWA

laser system is based on a Titanium-Sapphire system and consists of a phase-locked commercial oscillator (VITARA from COHERENT). The infrared (IR) pulse ($\lambda_0 = 788$ nm) are stretched and amplified in a regenerative amplifier. In a second stage, a multi-pass amplifier boosts the pulse energy to ~ 100 mJ. The IR pulses are finally compressed and converted to ultraviolet (UV, 263 nm) Fig. 1. The pulse shaper will be installed downstream of the oscillator and two pulse-characterization diagnostics will be implemented in the IR (for both the oscillator and amplifier IR pulse) and the UV. A

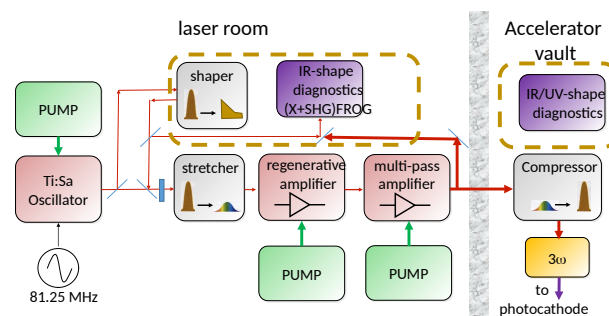


Figure 1: Overview of the AWA laser; see text for details.

femtosecond pulse from oscillator is shaped in a dispersive section with a Fourier transform pulse shaping scheme. The desired pulse shape can be obtained by manipulating the amplitudes or phases of different spectral components. For pulse characterization, a Frequency-Resolved Optical Gating (FROG) technique [7] is employed to measure the temporal distribution of the shaped pulses. Possible improvements of the setup are discussed.

LASER PULSE SHAPING

Laser pulse shaping has been an active field of research over the last two decades and has supported various scientific applications [8]. A number of shaping techniques have been implemented for ultrashort pulses [9]. Temporal shaping of a femtosecond pulse can be achieved via manipulation of its optical spectrum $\tilde{E}(\omega)$. The spectral amplitudes and phases of the input pulse are modified through a programmable digital to generate the desired output waveform $E(t)$.

A straightforward method to shape the spectrum of an ultrashort pulse consists in introducing a local spatial chirp using a dispersive element. A widely used setup is diagrammed in Fig. 2: a grating introduces the needed dispersion and a lens collimates the diverging beam. If the distances $a = b = f$ where f is the focal length associated to

* This work was supported by the US Department of Energy (DOE) contracts No. DE-SC0018656 with NIU and No. DE-AC02-06CH11357 with ANL.

[†] xu@niu.edu

the lens, the overall Kostenbauder matrix [10] of the shaper in (x, x', t, f) is $M = \begin{pmatrix} -I & 0 \\ 0 & I \end{pmatrix}$ where I is the identity matrix.

Therefore, such a system only introduces a spatial reflection in the dispersive plane while the vertical plane (y, y') remains unaffected. The transfer matrix from upstream of the grating to the mask is such that the spatial separation of the frequencies at the mask is $x_{mask} = D\omega - \omega_0$ where D is the spatial dispersion at the mask and ω_0 the central frequency associated with the pulse. The mask will affect the spectrum and consequently the temporal distribution of the pulse. Unfortunately for picosecond-scale laser pulses, such as needed to mitigate space-charge effects during the emission process, we have to introduce a chirp so that the frequency is proportional to time. With such a correlation, shaping the spectrum directly affects the temporal shape of the pulse [3]. Most generally the impact of the mask can be described by

$$\tilde{E}_{out}(\omega) = M(\omega)\tilde{E}_{in}(\omega) \quad (1)$$

where $M(\omega)$ describes the complex transfer function associated with the mask, and $\tilde{E}_{in}(\omega)$ and $\tilde{E}_{out}(\omega)$ denote the spectrum of input and output pulse. After the second lens and grating recombine all spectral components so that a temporally-shaped pulse is formed.

Figure 3 shows a simulated shaping process where a pulse with a Gaussian spectral profile ($\lambda_0 = 788\text{nm}$, FWHM = 26nm) is shaped into an asymmetric skewed Gaussian distribution. The spectral phase of the pulse is correlated with frequency after the pulse passes through a 2-cm BK7 glass. A spatial mask is then applied to the spectrum in which half of the spectral components are blocked. The temporal distribution of original and shaped pulse are compared in Fig. 3(d). In this specific case, the bandwidth is significantly decreased so that the final temporal pulse width is larger than the initial pulse. A higher degree of control can be achieved by properly controlling the mask parameter. The main options for the mask include liquid-crystal spatial light modulators and deformable mirrors. Both types of device are available in either one- or two-dimensional arrays and in-

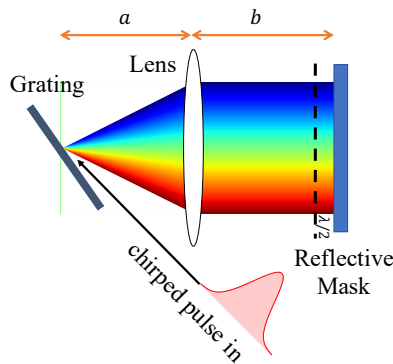


Figure 2: Basic setup for Fourier transform optical pulse shaping.

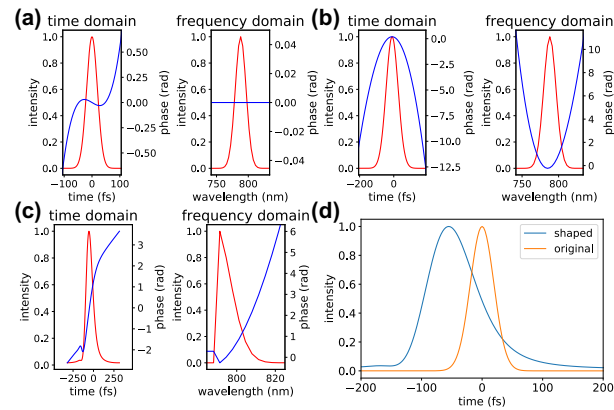


Figure 3: Simulation of a pulse shaping process. Time domain and frequency domain intensity and phase associated with the initial pulse (a), after propagation through a thick BK7 element (b), and downstream of the shaper (c). Comparison of the time-domain amplitude associated with the original and shaped pulses (d).

duce a controllable phase shift. We will use a 1-D nematic liquid-crystal SLM consisting of 12k addressable vertical strips (procured from BNS now available from Meadowlark). The SLM will be used in a folded-shaper configuration depicted in Fig. 2. The mask will be set up using an iterative algorithm guided by a measurement of the pulse temporal shape. In addition to this main research, we will investigate potential alternative configurations of the shaper including the use of cheaper alternative such as digital micromirror devices (instead of the SLM). The latter digital micromirror devices (DMD) could also be applied in the UV and provide direct control of the UV pulse shape. Likewise using the DMD and SLM in the IR could open the path to spatio-temporal shaping and/or control of the spectral amplitude and phase.

In practice, aberrations in the spectral phase will distort the output pulse shape. Also, nonlinear elements in the downstream optical setup, e.g., amplifiers, will alter the pulse temporal profile. Such effects can be accounted for by programming a mask transfer function capable of precorrecting the expected distortions. Setting the transfer function can also be done as part of a feedback system while monitoring the final temporal distribution.

ULTRASHORT LASER PULSE CHARACTERIZATION

The shape of a laser pulse can be defined by its electric field $E(t)$ or the corresponding $\tilde{E}(\omega)$. Direct measurement of the temporal profile of laser pulses using electrical detectors is limited to the picosecond range due to their relatively slow response time. FROG was introduced over two decades ago to overcome this limitation and are widely used to reconstruct pulse amplitude and phase. The most common variant of FROG utilizes the non-linear optical process of second harmonic generation (SHG). The idea is to temporally gate

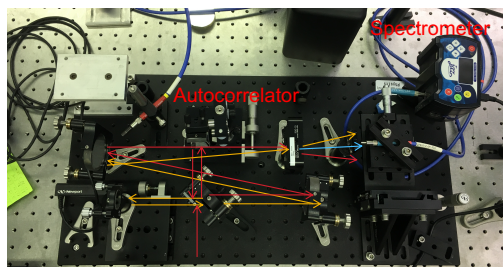


Figure 4: Optical setup of SHG-FROG at AWA.

the input pulse $E(t)$ with its delayed replica $E(t - \tau)$ and spectrally resolve the signal. This gives the two-dimensional measurement,

$$I_{\text{FROG}}^{\text{SHG}}(\omega, \tau) = \left| \int_{-\infty}^{\infty} E(t)E(t - \tau) \exp(-i\omega t) dt \right|^2, \quad (2)$$

where $I_{\text{FROG}}^{\text{SHG}}(\omega, \tau)$ is often referred as the SHG-FROG trace. It has been shown that there is a one-to-one correspondence between pulse field $E(t)$ and its FROG trace [11]. An iterative algorithm can then be used to reconstruct pulse field $E(t)$ from the FROG trace.

At AWA, an SHG-FROG device (Fig. 4) has been set up to measure the femtosecond pulses from laser oscillator. The pulse profile is retrieved using PYPRET package [12]. An example of measurement appears in Fig. 5. The spectrum of the original pulse was also measured upstream of the SHG FROG to validate the accuracy of the reconstructed spectral intensity $I(\omega)$. The FWHM of the retrieved pulse is 82 fs. The discrepancy between the reconstructed and measured spectrum could be attributed to misalignment in the setup limited bandwidth of some elements and will be further investigated once the laser is fully upgraded.

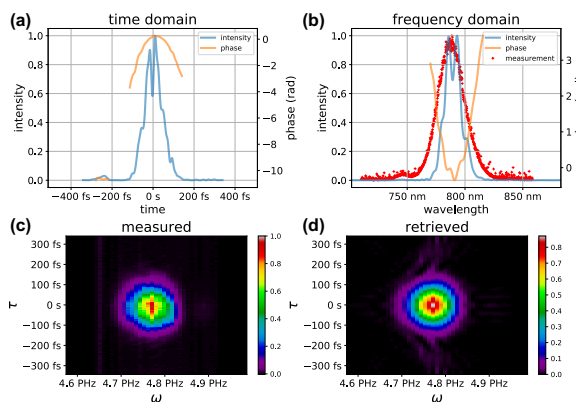


Figure 5: (a) Retrieved pulse distribution in the time domain. (b) Retrieved pulse distribution in the frequency domain. (c) Measured SHG-FROG trace. (d) Retrieved SHG-FROG trace.

The SHG FROG will be used to characterize the IR optical pulse downstream of the oscillator and amplifier chain. A polarization-gating (PG) FROG is under consideration for the UV pulse.

CONCLUSION

Shaping and characterization of photocathode lasers are critical to photoinjector generation of tailored electron bunches. In this paper, we described the setup for a Fourier-transform-based laser shaper. From the presented results we simulated the production of a quasi-triangular laser pulse using a spatial mask. For pulse characterization, preliminary measurement results from an SHG-FROG are presented. An integrated laser shaping and diagnostics system for precise pulse shape control are currently being developed.

REFERENCES

- [1] K. L. Bane, P. Chen, and P. B. Wilson, "On collinear wake field acceleration," in *Proc. 11th Particle Accelerator Conf. (PAC'85)*, Vancouver, BC, Canada, May 1985, pp. 3524–3526. doi: 10.1109/TNS.1985.4334416.
- [2] F. Lemery and P. Piot, "Tailored electron bunches with smooth current profiles for enhanced transformer ratios in beam-driven acceleration," *Phys. Rev. Spec. Top. Accel. Beams*, vol. 18, no. 8, p. 081301, 2015.
- [3] I. Kuzmin *et al.*, "Shaping triangular picosecond laser pulses for electron photoinjectors," *Laser Phys. Lett.*, vol. 16, no. 1, p. 015001, Nov. 2018. doi: 10.1088/1612-202x/aaef95.
- [4] T. Xu, C. Jing, A. Kanareykin, P. Piot, and J. Power, "Optimized electron bunch current distribution from a radiofrequency photo-emission source," in *Proc. 2018 IEEE Advanced Accelerator Concepts Workshop (AAC)*, Breckenridge, CO, USA, Aug. 2018, pp. 1–5. doi: 10.1109/AAC.2018.8659440.
- [5] F. Liu, S. Huang, S. Si, G. Zhao, K. Liu, and S. Zhang, "Generation of picosecond pulses with variable temporal profiles and linear polarization by coherent pulse stacking in a birefringent crystal shaper," *Opt. Express*, vol. 27, no. 2, pp. 1467–1478, 2019.
- [6] A. M. Weiner, "Femtosecond pulse shaping using spatial light modulators," *Rev. Sci. Instrum.*, vol. 71, no. 5, pp. 1929–1960, 2000.
- [7] D. J. Kane and R. Trebino, "Characterization of arbitrary femtosecond pulses using frequency-resolved optical gating," *IEEE J. of Quantum Electron*, vol. 29, no. 2, pp. 571–579, 1993.
- [8] A. Monmayrant, S. Weber, and B. Chatel, "A newcomer's guide to ultrashort pulse shaping and characterization," *Journal of Physics B: Atomic, Molecular and Optical Physics*, vol. 43, no. 10, p. 103001, 2010.
- [9] A. M. Weiner, "Ultrafast optical pulse shaping: A tutorial review," *Optics Communications*, vol. 284, no. 15, pp. 3669–3692, 2011.
- [10] A. G. Kostenbauder, "Ray-pulse matrices: A rational treatment for dispersive optical system," *IEEE Journal of Quantum Electronics*, vol. 26, no. 6, pp. 1148–1157, 1990. doi: 10.1109/3.108113.
- [11] R. Trebino and D. J. Kane, "Using phase retrieval to measure the intensity and phase of ultrashort pulses: Frequency-resolved optical gating," *J. Opt. Soc. Am. A*, vol. 10, no. 5, pp. 1101–1111, 1993.
- [12] N. C. Geib, *Python for pulse retrieval*, <https://github.com/ncgeib/pypret>, 2019.